IL NUOVO CIMENTO Vol. 31 C, N. 5-6 Settembre-Dicembre 2008
DOI 10.1393/ncc/i2009-10357-0

Experiments in stratified and rotating decaying 2D flows

A. Matulka([1])([2]), J. M. Redondo([1]) and J. A. Carrillo([1])

([1]) *Departamento de Física Aplicada, U.P.C. Campus Nord - Barcelona 08034, España*
([2]) *Warsaw University of Technology - Warsaw, Poland*

(ricevuto il 20 Dicembre 2008; approvato il 10 Marzo 2009; pubblicato online il 22 Luglio 2009)

Summary. — Two sets of turbulence decaying experiments have been performed, with the aim of focusing in the middle of a strongly stratified density interface. The experiments have been done under two different external conditions: a) stirring (non-rotating) decaying 2D turbulence experiments and b) rotating decaying 2D turbulence experiments. Non-rotating experiments were performed in a 1×1 m tank, while the rotating experiments were performed in a rectangular tank of 4×2 m; this rectangular tank was placed in the middle of the Coriolis rotating platform from the Trondheim Marine Systems Research Infrastructure supported by the European Community TMR Project. The set of stirred experiments is a compilation of five series of mixing experiments, dependent on the initial interfacial Richardson number. The total time of mixing was between 53 and 72 minutes. The density of the brine used in the experiment after was between 1027 and 1037 kgm^{-3}. The boundary conditions for all the rotating experiment are related to initial Reynolds *Rer*, Rossby *Ro*, Ekman *Ek* and Richardson gradient *Rig* numbers, the results are summarized and presented in a 3D parameter map using potential relationships.

PACS 47.27.-i – Turbulent flows.
PACS 47.27.De – Coherent structures.
PACS 47.55.Hd – Stratified flows.
PACS 47.32.Ef – Rotating and swirling flows.

1. – Introduction

Many experimental studies have been devoted to the understanding of non-homogeneous turbulent dynamics. Activity in this area intensified when the basic Kolmogorov self-similar theory was extended to two-dimensional or quasi 2D turbulent flows such as those appearing in the environment, that seem to control the ocean mixing in coastal areas. The statistical description and the dynamics of these geophysical flows depend strongly on the distribution of long-lived organized (coherent) structures in the atmosphere and the ocean (fig. 1). These flows show a complex topology, but may be subdivided in terms of strongly elliptical domains (high vorticity regions), strong hyperbolic domains (deformation cells with high-energy condensations) and the background

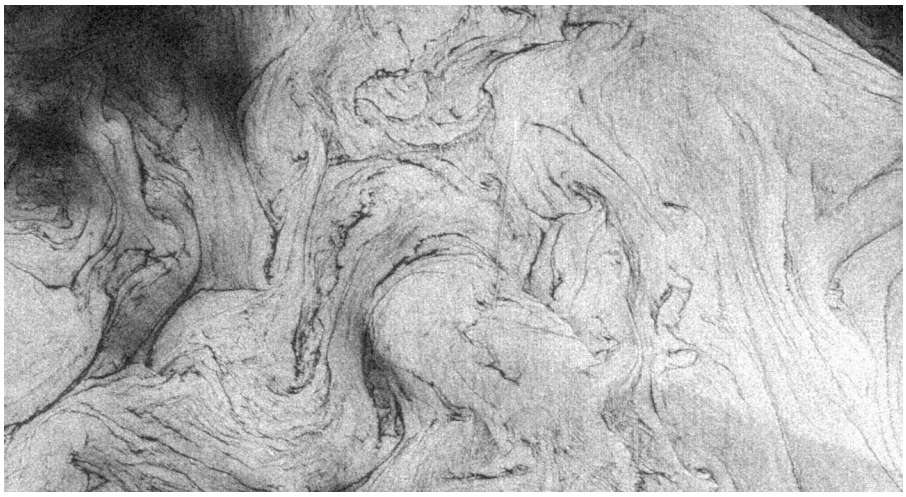

Fig. 1. – Coherent structures in the NW Mediterranean Sea, image of 60×35 km at 80 km from the Creus cape on 08 Jan. 1998. *Courtesy of A. Platonov.*

turbulent field of moderate elliptic and hyperbolic characteristics. It is of fundamental importance to investigate the different influence of these topological diverse regions on the eddy diffusivity. The scalar concentration of pollutants (tracers) within the flow will also be analyzed in the same fashion.

Experiments performed by [1-7] showed the effect of mixing from the edge on a rotating stratified system. When the instability is caused by differential heating or by buoyancy there seems to be a range of very different dynamic regimes, that may be detected in several different experiments: the zonally-symmetric circulation (ZC), anticyclonic gap-scale vortex (AGV), azimuthal wave/vacillation regimes (WR), and geostrophic turbulence regimes (GT).

The information needed to understand the pattern formation in these complex flows may be obtained from laboratory experiments on mixing in stratified and/or rotating fluids. This is essential for the development of computer models of geophysical phenomena, because, if better predictions are to be made, the distributions of potential and kinetic energy have to be correctly assessed for each process under study.

Following the work developed by [2, 1], this paper shows further analysis by means of experimental fluid dynamics and a detailled analysis of turbulence statistics and turbulent structures in rotating and stratified flows. The experiments have been performed at the Fluid Dynamics Laboratory of the Applied Physics Department of the UPC in Spain for the non-rotating stratified grid flows. The rotating stratified turbulence structure experiments presented here were made at the SINTEF laboratory in Trondheim Norway thanks to a Large Installation European Union Grant (HIDRALAB II).

This paper is organized as follows: sect. **1** gives a general view of the interesting problem of 2D turbulence and quasi-2D stratified (non-rotating) decay; in sect. **3** we describe the dimensional analysis and the relevant numbers used to characterize the presented experimental work. Next for the two main kinds of experiments, reported here, we describe the experimental set-ups and details of the visualization and analytical techniques used, these are presented in sect. **2**. The most important results and the

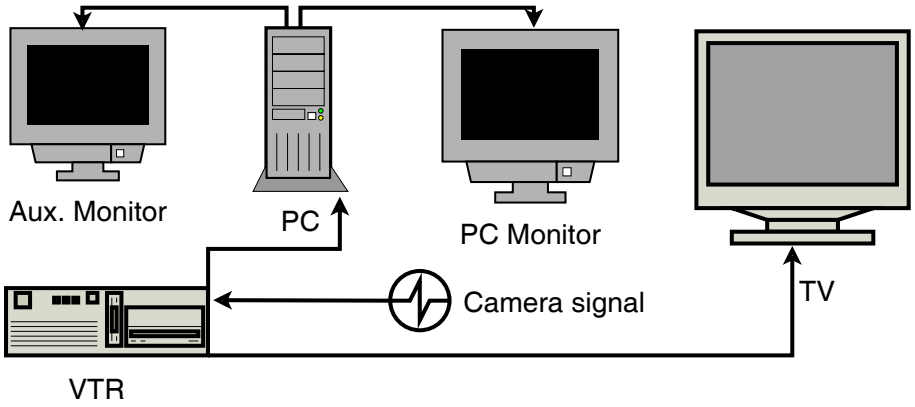

Fig. 2. – Image signal flow diagram from the experimental set-up.

available data for analysis are presented and discussed in sect. **4**. Finally, in sect. **5** we present the conclusions and some of the new methods developed to measure and explain the dynamics of 2D environmental turbulence.

2. – Description of the experiments

As the two sets of decaying turbulence experiments were stratified, we prepared previously to the grid stirring a two layer system by pouring carefully water on top of brine and focused the analysis on the horizontal motions in the middle of the density interface. At this location, plastic particles of pliolite were placed as the tank filled; in order to ensure the particle's position, they were previously treated in salty water to have neutral buoyancy in the interface. Side shadowgraph was used, taking advantage of the change in the refractive index to detect the interface laden with pliolite particles. In all experiments a thin horizontal layer at the height of the density interface was lit up by means of a powerful arc lamp and collimated by a slit in a dark screen. Experiments will be described and discussed in two basic categories: a) non-rotating decaying 2D turbulence experiments (with no rotation, *i.e.* $\omega = 0$) and b) rotating decaying 2D turbulence experiments. The stratification was measured in terms of the Brunt-Väisälä frequency at the interface N.

2˙1. *Visualization techniques*. – All the experiments were recorded by a video camera. The signal was then also digitalized by a DT-2861 data translation frame grabber and a personal computer with the fluid mechanics package DigImage [3, 4]. Figure 2 shows in a flux diagram the image analysis configuration. It allowed to work in real time on both TV and monitor where the processed images were visualized.

Filter, contouring, particle streaks and some other geometrical operations were applied using the facilities provided by the software to measure the advance of the turbulent interface (from side images) and the evolution of the dominant length scales and the spectral behavior from the top views of the density interface.

2˙2. *Non-rotating decaying 2D turbulence experiments*. – A set of five series of experiments was performed on a square tank of dimensions 1×1 m. This tank (fig. 3) was filled up to 10 cm (100 liters of water), 5 cm of them with salty water of different

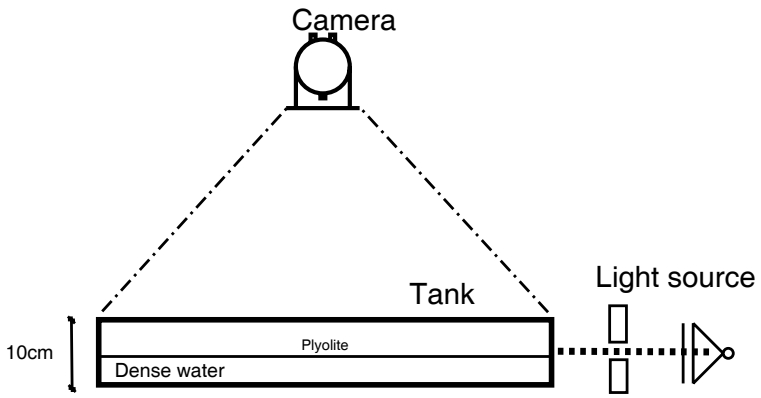

Fig. 3. – Lateral view of the experimental 1×1 m tank. A density interface with 5 cm of salty water and 5 cm of clean water was created. Carefully a third layer of plastic plyolite particles was placed in the middle of the salty and the clean waters.

concentration and the top 5 cm with fresh water. Between these two layers, as mentioned above a thin layer (of about 1 cm) was seeded with the plastic particles of pliolite, marking the flow at the layer which separated brine and fresh water. In order to mix these two layers, a horizontally traversing grid (fig. 4) was used, pulling it at near constant velocity with the help of railings. The grid was built from thick plastic coated aluminium pipe sections held by a transversal aluminium holder. The bar centres were placed every 10 cm, their length being 30 cm and their diameter 3.5 cm. This configuration ensured a well-controlled strong initial vorticity produced by the Karman vortices of the round pipe array.

This experiment had five subsets arranged in terms of the different initial density difference at the interface before the experiments started. Before and after each one of the experiments, measurements of the density profiles were obtained from point measure-

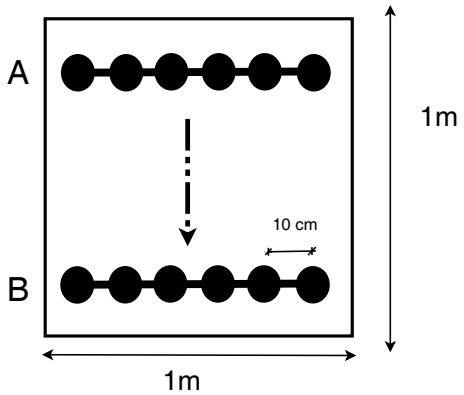

Fig. 4. – Diagram of the decaying turbulence experiments in the 1×1 m tank. Where a traversing grid of 30 cm with bars of 3.5 cm of diameter, separated by 10 cm, moved from A to B at a time of Δt.

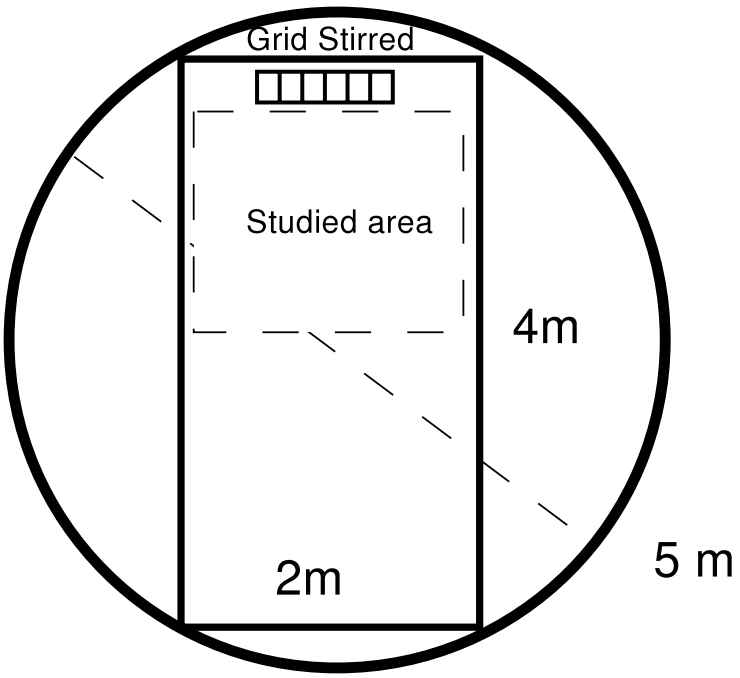

Fig. 5. – Rectangular tank of 4×2 meters placed in the center of the turntable of 5 m diameter and of 50 cm depth. Where experiments of decaying 2D turbulence with grid stirred were performed.

ments at different heights chosen as 1, 3, 5, 7, 8, 9 and 10 cm height, several points inside the tank were measured to ensure uniformity. Every experiment had a different salinity profile and quite linear sections at the centre of the brine fresh water interface. All measurements used calibrated conductivity probes and refractometer on a small drawn sample to be able to check on mass conservation. The measurements for each set consisted on seven or eight profiles between the different passages of the grid. The mixing efficiency was measured between passages and it was related with the increase of potential energy and the decay process considering how long and how many grid passages were necessary for these two layers to be totally mixed. The kinetic energy of the grid available for mixing was calculated from its drag coefficient. To consider individual turbulent decay processes in order to study the mixing process the grid was driven through the interface with the bars parallel to the interface and then we waited until all motions stopped. After this the densities were measured in the seven points and repeating the whole procedure again until the density in the whole tank was uniform.

2˙3. *Rotating decaying 2D turbulence experiments.* – A total of 63 experiments were performed on a rectangular tank of 4×2 m, this tank was in the center of the Coriolis tank (or turntable that had a diameter of 5 m and a depth of 50 cm (fig. 5)). The Coriolis tank is part of the SINTEF Trondheim Marine Systems Research Infrastructure supported by the European Community by HIDRALAB II. This set-up had been used to simulate rotating decaying turbulence and similar observations in a horizontal 2D plane.

In the center of the tank at two meters height a video camera was placed. The experiments were then filmed and recorded by a SVHS video following the procedure described in subsect. **2˙1**.

The aim of this set of rotating-stratified experiments was to perform a parametric investigation in the *Re-Ro* field, with conditions as varied as possible, considering the limitations of the Coriolis platform and the practical range of density differences and grid velocities. This large experimental data set was designed in order to describe with aid of full velocity and vorticity PIV and particle tracking methods the structure of the turbulence and its topology under those varied parametric conditions in rotating and stratified flows.

3. – Basic equations

In order to compare experience between different works, dimensionless parameters must to be used. Some of its are the Gradient Richardson, Rossby and Reynolds numbers. Those numbers can be found in several books with a level similar to [5].

3˙1. *Gradient Richardson number (Rig).* – The basic nondimensional parameter that describes the effects of stratification in stable situation is the Richardson number, it can be described as gradient Richardson (Rig) or as flux Richardson (Rif) numbers. Rif relates buoyancy flux to turbulent production by shear or the other causes, while Rig [8,9], a simpler parameterization of the effects of buoyancy, is often used to indicate the stability of the shear flows, it relates the variables that control the mixing at interface as follows:

$$Rig = \frac{g}{\rho} \frac{\partial \rho / \partial z}{(\partial u / \partial z)^2} , \tag{1}$$

where the natural buoyancy frequency often named Brunt-Väisälä explained as

$$N = \left(-\frac{g}{\rho} \frac{\partial \rho}{\partial z} \right)^{1/2} \tag{2}$$

includes the density gradient $\partial \rho / \partial z$, as a main mixing controller at the interface. Here g and ρ are the averaged fluid gravity and density, respectively.

3˙2. *Ekman number (Ek).* – As the numbers used in this paper, the Ekman number is used to describe effects in oceans and atmosphere phenomena. Formally it is described as

$$Ek = \frac{\nu}{f L^2} , \tag{3}$$

where ν is the kinematic eddy viscosity, f is the Coriolis parameter and L is the relevant eddy length scale.

3˙3. *Rossby number (Ro).* – The basic non-dimensional parameter used to describe the effects of rotation is the Rossby number considered as the ratio of the local fluid induced vorticity to the part of the absolute vorticity induced by the overall external rotation.

$$Ro = \frac{Fr}{f} , \tag{4}$$

TABLE I. – *Initial conditions from the stirred experiments, velocity u, Brunt-Väisäla frequency N and the dimensionless numbers Reynolds Re and Richardson gradient Rig.*

u (ms^{-1})	N (s^{-1})	Re	Rig
0.24	0.75	24×10^3	0.09
0.22	0.46	22×10^3	0.03
0.20	0.48	20×10^3	0.05
0.40	0.48	40×10^3	0.01

where $Fr = 4\,\mathrm{Hz}$ is the grid stirred frequency and f is the Coriolis parameter defined as $f = 2\Omega$.

3˙4. *Rotating Reynolds number (Rer).* – In order to obtain a compromise between the experimental, numerical and natural conditions, the rotating (or rotation) Reynolds number is used following

$$Rer = \frac{\Omega h^2}{\nu}\,, \tag{5}$$

where Ω is the angular speed, h is the representative depth and ν is the kinematic viscosity. It is necessary to mention that the used Reynolds in the stirred experiments is the regular expression $Re = uL/\nu$, where u and L are the characteristic velocity and length scales, respectively.

4. – Results and discussion

4˙1. *Non-rotating stratified experiments.* – The set of experiments is a compilation of five sub-sets of total mixing experiments labeled as 1 to 5. The basic parameter used to compare them was the initial Richardson number. The total time for complete mixing was between 53 and 72 minutes, so diffusive molecular mixing of salt was negligible in all cases. The density of fluid after total mixing was in the range between 1027 and 1037. This differences were due to the fact that the experiments had different initial densities, in all cases mass conservation was ensured by calculating it from the average density profiles. This differences in initial density profiles and in grid forcings (10–40 cm/s) produced a wide range of mixing efficiencies. This paper will discuss in detail four experiments which are identified by the initial Gradient Richardson number Rig. Initial conditions of u, N, Re and Rig from the stirred experiments are shown in table I. Two of those experiments had profiles shown as a and b in fig. 6.

Figure 7 shows a time series of density profiles from the experiments with $Rig = 0.09$ and $Rig = 0.03$.

The grid stirred experiments viewed from the top show their development in fig. 6 corresponding to the experimental set number 3. For each pair of profiles (from a to i), their corresponding increase in potential energy is calculated as

$$\Delta PE = \int z(\rho_{\mathrm{after}}(z) - \rho_{\mathrm{before}})\mathrm{d}z, \tag{6}$$

it represents the mixing produced during a single experiment of turbulent decay. For instance, fig. 8 shows Rig experiments 0.09 and 0.03.

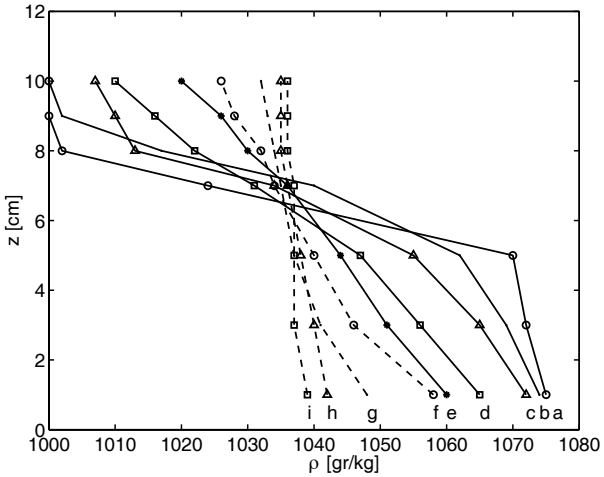

Fig. 6. – Total mixing experiments with NaCl from a with a lower layer $\rho = 1075$, throughout b, c, d... until i. The totally mixed (i) density in this experiment was $\rho = 1037$. The discontinuous lines indicate experiments with weak stratification and low Rig.

4˙1.1. Dimensionless time and length scales. As the stratification produces a complex interaction between the vertical vorticity produced by the collapse of the eddies and the horizontal vorticity produced by breaking internal waves with strong local vertical displacements at the density interface the homogeneous 2D turbulence decay power law is not going to be followed, even in the strongly stratified situations. For the very weakly stratified flows we expect that the integral scale, or length scale where most kinetic energy resides, will not decay as fast and follow a 3D decay. We have to choose between different forcing and internal parameters to construct the dimensionless numbers that we are looking for, so we may distinguish different scaling effects during the whole mixing process. For example, we may compare similar behaviors under different conditions, characterized by different scales that may be useful in order to compare between natural large-scale and experimental (small-scale laboratory) flows. Here we will explore the relationship Time (T)-Integral length scale (L), scaled both with the grid forcing time scale and with the internal wave frequency time scale $1/N$. On the one hand, fig. 8 left shows the T-L relation (s and cm, respectively) indicating a power law close to $T^{3/5}$. On the other hand, fig. 8 right presented the dimensionless relationship T-L/M, where M is the characteristic grid scale equal to 10 cm. Note that in this case T may be adimensionalised in two ways: 1) T times the Brunt-Väisäla frequency (N) and 2) T times the characteristic velocity u divided by M. In both cases the dominant relationship is proportional to $T^{3/5}$. But the kink in the growth law is a clear sign of the interactions between the dominant vortices and the internal waves. Note also that because the motions can also be vertical faster flowing crests of the internal waves are detected in the flow visualizations. The velocity at the plane intersecting several times a set halocline does not have to comply with the continuity equation. See, for example, fig. 9.

4˙2. *Rotating stratified experiments.* – The experimental domain related to dimensionless numbers is very important to relate experimental results with natural and numerical models. The boundary conditions from all the rotating experiment conditions related to

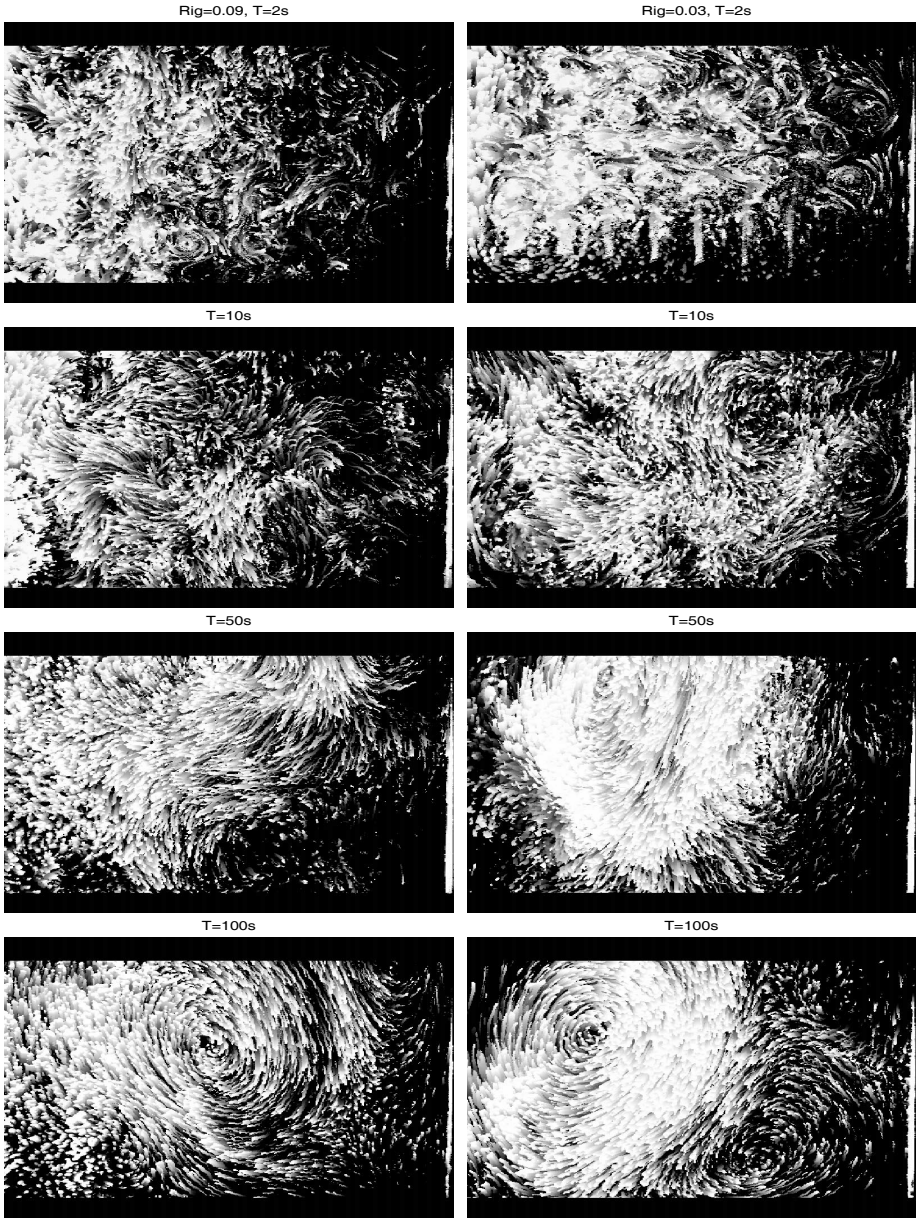

Fig. 7. – Experiment time series with *Rig* equal to 0.09 (left) and 0.03 (right), at times 2, 10, 50 and 100 seconds. Note the evolution of the size of the vortex from small at the beginning to large at the end.

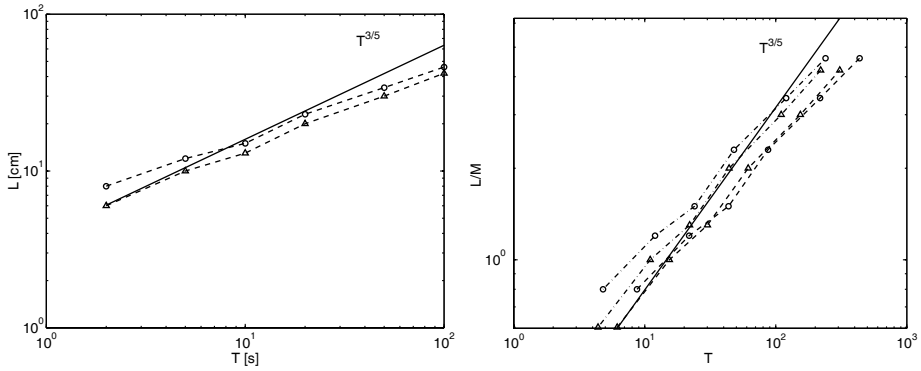

Fig. 8. – Experiments with Rig equal to 0.09 (o) and 0.03 ($\triangle$) from left: The different characteristic scales L(cm) according to time T(s), and right: dimensionless expression of L/M and $T \times N$ (- -) and Tu/M (-.-), where M and u are the characteristic grid length scale (10 cm) and velocity, respectively.

rotating Reynolds Rer, Rossby Ro, Ekman Ek and Richardson gradient Rig numbers are summarized in table II.

Dimensionless numbers are related to the balance of the different forces implicated in the flows. For instance the rotating Reynolds number, set here, relates the inertia forces due to rotation against the kinematic viscosity forces; the Rossby number relates the local vorticity against the total vorticity in the whole domain (this case experimental); the Ekman number relates the eddy viscosity forces against the rotational eddy forces

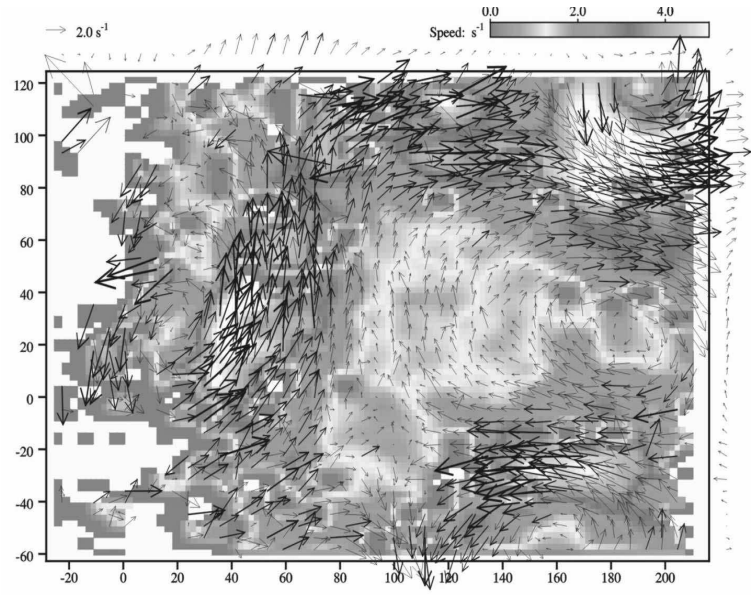

Fig. 9. – Lagrangian velocity field in the non-rotating decaying 2D turbulence. This frame shows the structures presented with $Rig = 0.03$ and $T = 10$ seconds.

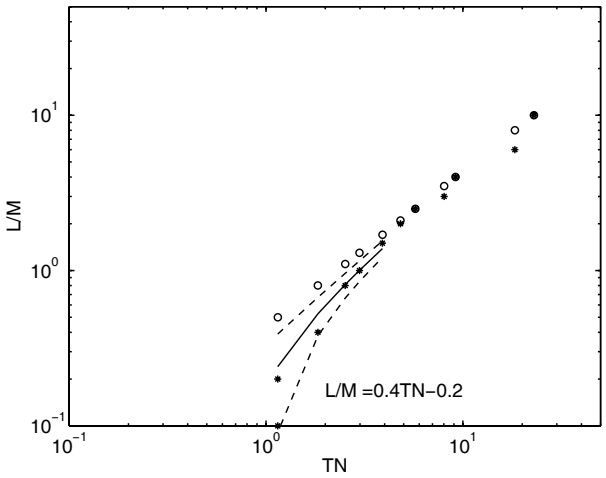

Fig. 10. – Dimensionless domain of $T \times N$ *vs.* dimensionless expression L/M, where $M = 10\,\text{cm}$.

and the Richardson gradient number compares the buoyancy force against the inertia induced by shear. Figure 10 shows in a non-dimensional way in log-log coordinates that the role of different stratifications is dominant before Nt reaches the value of 5.

4˙2.1. Dimensionless parameter fields. The set of rotating experiments presented a dependence between both *Rer* and *Rig* (see fig. 11 right), while *Rer* did not presented such clear dependence with *Ro* (fig. 12 left) and *Ek* (fig. 12 right) numbers. At the same time, *Ro* did not showed any clear dependence with *Rer* (fig. 11 left) because of the varied conditions used so that equilibrium between rotation and stratification was not reached within the time span of many of the experiments.

The dependence between *Rer* and *Rig* was seen to be proportional to $Rer^{-3/4}$; this is due to the fact that in both numbers, the inertia is a relevant component. This result is slightly different from that found by [2] in a natural narrow estuary where the relationship was proportional to $Re^{-3/2}$ and rotation was not relevant.

Figure 13 shows the same characteristic values for the rotating stratified experiments on a three-dimensional parameter space. The dimensional relationship between the gradient Richardson number and the Reynolds number, which is modified due to the dependence of the length scale associated to the interface thickness as indicated in [10] $\propto Rig^{-2/3}$, groups the available experiments around the elongated region as seen in fig. 13.

TABLE II. – *Experimental domain related to the dimensionless numbers Reynolds Rer, Rossby Ro, Ekman Ek and Richardson gradient Rig.*

Number	From	Until
Rer	2500	1.6×10^{6}
Ro	0	32.5
Ek	0	4.8×10^{-6}
Rig	0	1.6×10^{5}

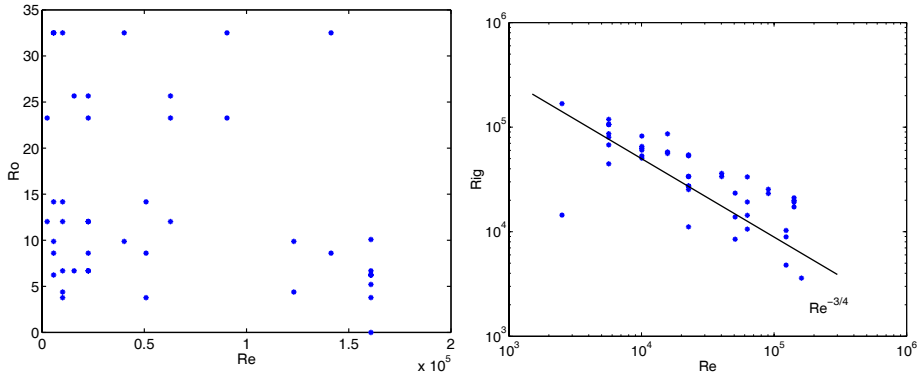

Fig. 11. – Parametric field in the rotating decaying 2D turbulence experiments performed in the Coriolis tank. Left: *Re-Ro* and right: *Re-Rig*, note the dependence of both *Rig* and *Re* on the characteristic velocity.

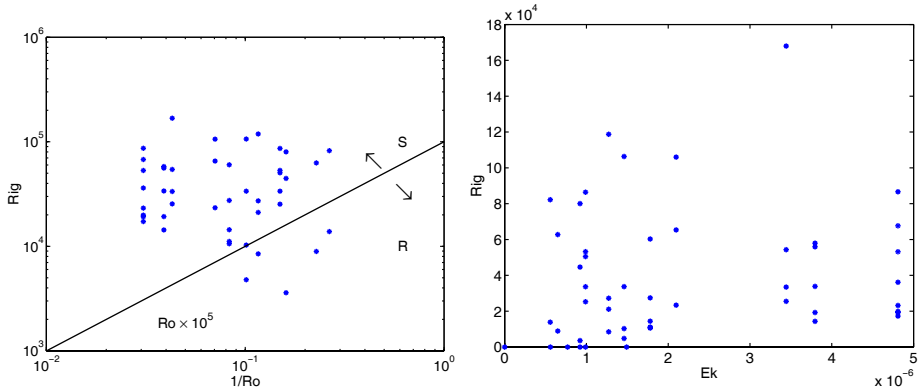

Fig. 12. – Parametric field in the rotating decaying 2D turbulence experiments performed in the Coriolis tank. Left: *Ro-Rig* and right: *Ek-Rig*. *R* indicates the parameter space dominated by rotation and *S* indicates the parameter space is dominated by stratification (buoyancy forces).

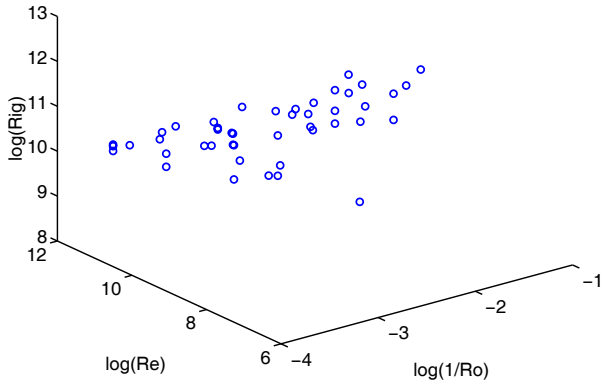

Fig. 13. – Experimental 3D parametric field from *Ro*, *Re* and *Rig* from the rotational experiments performed in the Coriolis table at the *SINTEF* laboratory.

In the cases where the experimental initial conditions were spread out across all the parametric fields (values showed in table II) they obeyed to the fact that we specifically looked for the largest possible variability in the range of parameters that the experimental facilities made possible to work with.

The results of this paper are designed to show the extent of the available data developed by the authors within the HIDRALAB II project. Detailed analyses of the data with new methods of PIV and conditional sampling in the field of stratified and rotating flows have been developed and are available for further exploration of the different parametric regions. For instance, processing velocity data of the grid experiments is under way using structure function and intermittency analysis.

The set of rotating stratified experiments may be classified in regions dominated by one or several dominant instabilities such as those appearing in the non-rotating case [10] internal waves, Holmoe instability, Kelvin-Helmholtz billows, non-linear pairing and fully developed turbulence.

In the case of rotating stratified flows, instead of using the Burger number, because the equilibrium between rotation and stratification is attained when $RiRo = 1$, we may use the diagonal to conditionally sample the different scales of the Rossby deformation radius $R_D = Nh/f$ when R_D are stable. A new parameter map to be used as a general frame of reference with Rig, $1/Ro$ and Rer presents important advantages when comparing different experiments and field data, and simplifies the complicated relationship between these dimensionless numbers.

5. – Conclusion

The analyzed stirred experiments were performed under the initial conditions from $Re = 24 \times 10^3$ and 22×10^3; $Rig = 0.46$ and 4.75; and $N = 0.75$ and 2.65. The relationships T-L, TN-L/M and Tu/M-L/M were proportional to $T^{3/5}$ from the non-rotating experiments.

From the rotating experiments, analysis with parametric fields showed a dependence between Rer and Rig proportional to $Rer^{-3/4}$ different from that reported from natural conditions without rotation where the values were proportional to $Rer^{-3/2}$.

The parameter analysis showed a non-dependence between the rest of the dimensionless numbers and its values spread out across the values of Rer from 2500 to 1.6×10^6; Ro from 0 to 32.5; Ek from 0 to 4.8×10^{-6} and Rig from 0 to 1.6×10^5.

The expected sample dependence between Rig and Re is found eliminating the velocity between

$$Re = \frac{LV}{\mu} \qquad \text{and} \qquad Rig = \frac{N^2 L^2}{V^2}\,;$$

$$Rig = \frac{N^2 L^4}{\mu^2} Re^{-1/2}. \tag{7}$$

Note that

$$V = Re\frac{\mu}{L} => Rig = \frac{N^2 L^2}{Re^2 \frac{\mu^2}{L^2}} => Rig = \frac{N^2}{\mu^2} L^4 Re^{-1/2}$$

cannot be applied because of the modification of the vertical length scale due to both

stratification and rotation. This stresses the need of measuring the relevant length scale during the experiments.

As seen in the non-rotating experiments, there is a clear interaction between the internal wave field and the domain size of the horizontal vortices for non-dimensional times $NT < 5$. The final growth of the size of the decaying stratified vortices is controlled by the size of the experimental domain.

When there is an external imposed length scale, it can be shown, applying a simple equilibrium model as

$$\frac{\mathrm{d}k}{\mathrm{d}t} = \epsilon \propto K^{3/2}, \tag{8}$$

that the energy decays as $K(t) \propto t^2$, but the role of the initial conditions and the influence of the stratification, which would include an extra buoyancy term in eq. (8), modifies the evolution of both the turbulence kinetic energy and the domain scales.

The role of Coriolis-induced inertial waves as well as the buoyancy-induced internal waves is expected to influence most the inertial decay phase of the flow. So in order to modify global parameters as the mixing efficiency, the control of the initial conditions seems much more important than previously thought [8, 9]. The changes in local mixing efficiency in rotating and stratified affects the global behaviour of a whole estuary as shown by [1, 7, 11], knowing the basic instabilities as a function of the position in parametric space $(Re, Ri, 1/Ro)$ is important for environmental applications.

REFERENCES

[1] Carrillo J. A., Redondo J. M., Sánchez M. A. and Platonov A., *Phys. Chem. Earth*, **26** (2001) 305.

[2] Carrillo J. A., *Influencia de la Turbulencia y de la Dinámica de Interfases de Densidad Sobre Organismos Planctónicos: Aplicación al estuario del Ebro*, Ph.D. Thesis, UPC, Spain (2002).

[3] Dalziel S. B., *Appl. Sci. Res.*, **49** (1992) 217.

[4] Dalziel S. B., *Decay of rotating turbulence: some particle tracking experiments*, in *Flow Visualization and Image Analysis*, edited by Nieuwstadt F. T. (Kluwer, Dordrecht) 1993, pp. 27-54.

[5] Kundu P. K., *Fluid Mechanics* (Academic Press, NY) 1990.

[6] Linden P. F., Boubnov B. M. and Dalziel S. B., *J. Fluid Mech.*, **298** (1995) 81.

[7] Pérez M. C. and Carrillo J. A., *Acta Bot. Croat.*, **64** (2005) 237.

[8] Turner J. S., *J. Fluid Mech.*, **33** (1968) 639.

[9] Turner J. S., *Buoyancy Effects in Fluids* (Cambridge University Press, Cambridge) 1973.

[10] Redondo J. M., *The structure of density interfaces*, PhD, Cambridge University (1990).

[11] Carrillo A., Huq P., Pèrez M. C. and Redondo J. M., *Estuarine Coastal Shelf Sci.*, **78** (2008) 153.